In vivo production of psilocybin in *E. coli*

Alexandra M. Adams[a], Nicholas A. Kaplan[a], Zhangyue Wei[a], John D. Brinton[a], Chantal S. Monnier[a], Alexis L. Enacopol[a], Theresa A. Ramelot[b], J. Andrew Jones[a,*]

[a] *Miami University, Department of Chemical, Paper, And Biomedical Engineering, Oxford, OH, 45056, USA*
[b] *Miami University, Department of Chemistry and Biochemistry, Oxford, OH, 45056, USA*

ABSTRACT

Psilocybin, the prodrug of the psychoactive molecule psilocin, has demonstrated promising results in clinical trials for the treatment of addiction, depression, and post-traumatic stress disorder. The development of a psilocybin production platform in a highly engineerable microbe could lead to rapid advances towards the bioproduction of psilocybin for use in ongoing clinical trials. Here, we present the development of a modular biosynthetic production platform in the model microbe, *Escherichia coli*. Efforts to optimize and improve pathway performance using multiple genetic optimization techniques were evaluated, resulting in a 32-fold improvement in psilocybin titer. Further enhancements to this genetically superior strain were achieved through fermentation optimization, ultimately resulting in a fed-batch fermentation study, with a production titer of 1.16 g/L of psilocybin. This is the highest psilocybin titer achieved to date from a recombinant organism and a significant step towards demonstrating the feasibility of industrial production of biologically-derived psilocybin.

1. Introduction/background

Psilocybin (4-phosphoryloxy-*N,N*-dimethyltryptamine) has gained attention in pharmaceutical markets as a result of recent clinical studies. The efficacy of psilocybin has been demonstrated for the treatment of anxiety in terminal cancer patients (Belser et al., 2017; Grob et al., 2011; Ross et al., 2016) and alleviating the symptoms of post-traumatic stress disorder (Gluff et al., 2017; Johnson and Griffiths, 2017) (PTSD). Most recently, the United States Food and Drug Administration (U.S. FDA) has approved the first Phase IIb clinical trial (Moisala et al., 2017; Raison, 2019) for the use of psilocybin as a treatment for depression that is not well controlled with current available interventions such as antidepressants and cognitive behavioral therapies (Carhart-Harris et al., 2016; Grob et al., 2011; Johnson and Griffiths, 2017; Ross et al., 2016; Tylš et al., 2014). Psilocybin was first purified from the *Psilocybe mexicana* mushroom by the Swiss chemist, Albert Hofmann, in 1958 (Hofmann et al., 1958; Passie et al., 2002). The first reports of the complete chemical synthesis of psilocybin were published in 1959 (Hofmann et al., 1959); however, large-scale synthesis methods were not developed until the early 2000's by Shirota and colleagues at the National Institute of Sciences in Tokyo (Shirota et al., 2003). Despite significant improvements over early synthetic routes, current methods remain tedious and costly, involving numerous intermediate separation and purification steps resulting in an overall yield of 49% from 4-hydroxyindole (Shirota et al., 2003), incurring an estimated cost of $2 USD per milligram for pharmaceutical-grade psilocybin (Fricke et al., 2019).

Many scientists are interested in psilocybin because of its biosynthetic precursors—norbaeocystin and baeocystin (Leung and Paul, 1968). These compounds have structural similarity to the neurotransmitter serotonin (Lin et al., 2014; Sun et al., 2015; van den Berg et al., 2010) and sparked the interest of researchers who were curious to understand the mechanism behind their hallucinogenic properties. After being named a Schedule I compound in the US with implementation of the Controlled Substance Act of 1970 (Johnson et al., 2018), research efforts involving psilocybin were abandoned for other less regulated bioactive molecules; however, experts in the field have suggested a reclassification to schedule IV would be appropriate if a psilocybin-containing medicine were to be approved in the future (Johnson et al., 2018).

Carhart-Harris and colleagues are conducting ongoing clinical trials with psilocybin as a medication for individuals struggling with treatment-resistant depression (Carhart-Harris et al., 2017, 2016). Treatment-resistant forms of depression represent about 20% of the 350

million cases of depression worldwide (Kessler et al., 2015). During the clinical trials, the medication is administered in a controlled environment, with a team of psychiatrists and psychologists guiding the patients through the psilocybin experience. After a single treatment, 42% of the patients were considered to be in remission, which was classified as having reported improved mood and reduced depressive symptoms for up to three months (Carhart-Harris et al., 2016). These promising results have motivated researchers to investigate biosynthetic routes for the production of psilocybin. The Hoffmeister group recently identified the enzymatic pathway from *Psilocybe cubensis* (a native fungal psilocybin producer) and demonstrated *in vitro* synthesis of psilocybin from 4-hydroxytryptophan (Fricke et al., 2017). In a subsequent work, they utilized the promiscuity of the tryptophan synthase from *P. cubensis* to make psilocybin from 4-hydroxyindole and serine (Blei et al., 2018). Additionally, the Hoffmeister group produced psilocybin *in vivo* using an eukaryotic fungal host, *Aspergillus nidulans*, at titers reported near 100 mg/L (Hoefgen et al., 2018). These breakthroughs in the biosynthesis of psilocybin have resulted in a newfound interest in understanding how to efficiently synthesize the promising and pharmaceutically-relevant molecule for the long-term treatment of multiple chronic disease that affect millions (Johnson and Griffiths, 2017).

These new advancements fueled our interest in developing a more cost-effective and easily manipulated host for the biosynthetic production of psilocybin. Utilizing the gene sequences recently identified by the Hoffmeister group from *P. cubensis* encoding an L-tryptophan decarboxylase (PsiD), a kinase (PsiK), and an S-adensoyl-L-methionine (SAM)-dependent N-methyltransferase (PsiM) (Fricke et al., 2017), together with the promiscuity of the native *Escherichia coli* tryptophan synthase (TrpAB) (Buller et al., 2015; Romney et al., 2017; van den Berg et al., 2010; Wilcox, 1974), the biosynthesis pathway capable of psilocybin production from 4-hydroxyindole, was expressed in the prokaryotic, model organism *E. coli* BL21 star™ (DE3) (Fig. 1d). For this proof-of-principle study, *E. coli* was chosen for the vast amount of metabolic knowledge and genetic tools available to assist in the engineering effort, unlike the limited set for *Aspergillus nidulans*. Psilocybin production was optimized through the application of a series of 3 parallel genetic optimization methods including: (1) a defined three-

level copy number library, (2) a random 5-member operon library, and (3) a random 125-member pseudooperon library. After transcriptional optimization methods were employed, the best strain, pPsilo16, underwent a thorough optimization of fermentation conditions, resulting in the production of ~139 ± 2.7 mg/L of psilocybin from 4-hydroxyindole. We conclude our work with a fed-batch bioreactor scale-up study, which resulted in the production of ~1160 mg/L of psilocybin, the highest titer reported to date from a recombinant host.

2. Results

2.1. Psilocybin production in E. coli

The previously confirmed psilocybin production genes (*psiD*, *psiK*, and *psiM*) from *P. cubensis* were heterologously expressed in *E. coli* using the strong T7 promoter system. Induction with IPTG allowed for the production of 2.19 ± 0.02 mg/L psilocybin. To confirm compound identities, culture media from our psilocybin production host was subjected to liquid chromatography-mass spectroscopy analysis on a Thermo Orbitrap XL LC-MS system. Psilocybin, as well as all precursor and intermediate compounds in the biosynthetic pathway, were identified with better than 5 ppm mass accuracy as shown in Fig. S3. The sample was then subjected to additional MS/MS fragmentation analysis to further support structural identification of all indole derived intermediates and final products. In each case, fragmentation products for the deamination, dephosphorylation (if applicable), and loss of both functional groups were observed, confirming the identification of psilocybin, and its intermediates: 4-hydroxytryptophan, 4-hydroxytryptamine, norbaeocystin, and baeocystin, with better than 5 ppm mass accuracy (Fig. S3). Additionally, expected retention times and order of elution were consistent with previously published efforts (Blei et al., 2018; Fricke et al., 2017). The overexpression of the native tryptophan synthase (TrpAB) was also performed in an attempt to push flux through the heterologous production pathway (data not shown). The native expression level was determined to be sufficient to maintain the necessary pathway flux, as supported by the buildup of 4-hydroxytryptophan in nearly all fermentation studies performed (Figs.
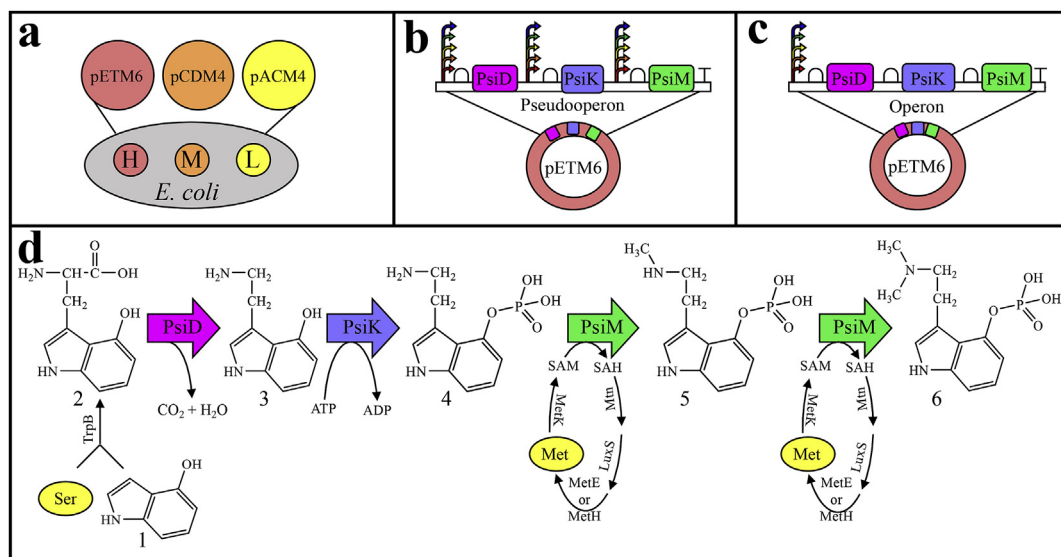

Fig. 1. Summary of library configurations and biosynthesis pathway. (a) Copy number library consisting of three plasmids with high (H), medium (M), and low (L) copy number, (b) Pseudooperon library consisting of a promoter in front of each gene with a single terminator on the high copy number plasmid, (c) Basic operon library consisting of one promoter in front of all three genes on the high copy number plasmid, and (d) Psilocybin biosynthesis pathway consisting of three heterologous enzymes, PsiD, PsiK, and PsiM, and highlighting the media supplements in yellow of serine and methionine (as described in methods). PsiD: L-tryptophan decarboxylase, PsiK: kinase, PsiM: S-adensoyl-L-methionine (SAM)-dependent N-methyltransferase, TrpB: tryptophan synthase beta subunit, Ser: serine, Met: methionine, 1: 4-hydroxyindole, 2: 4-hydroxytryptophan, 3: 4-hydroxytryptamine, 4: norbaeocystin, 5: baeocystin, 6: psilocybin. (For interpretation of the references to color in this figure legend, the reader is referred to the Web version of this article.)
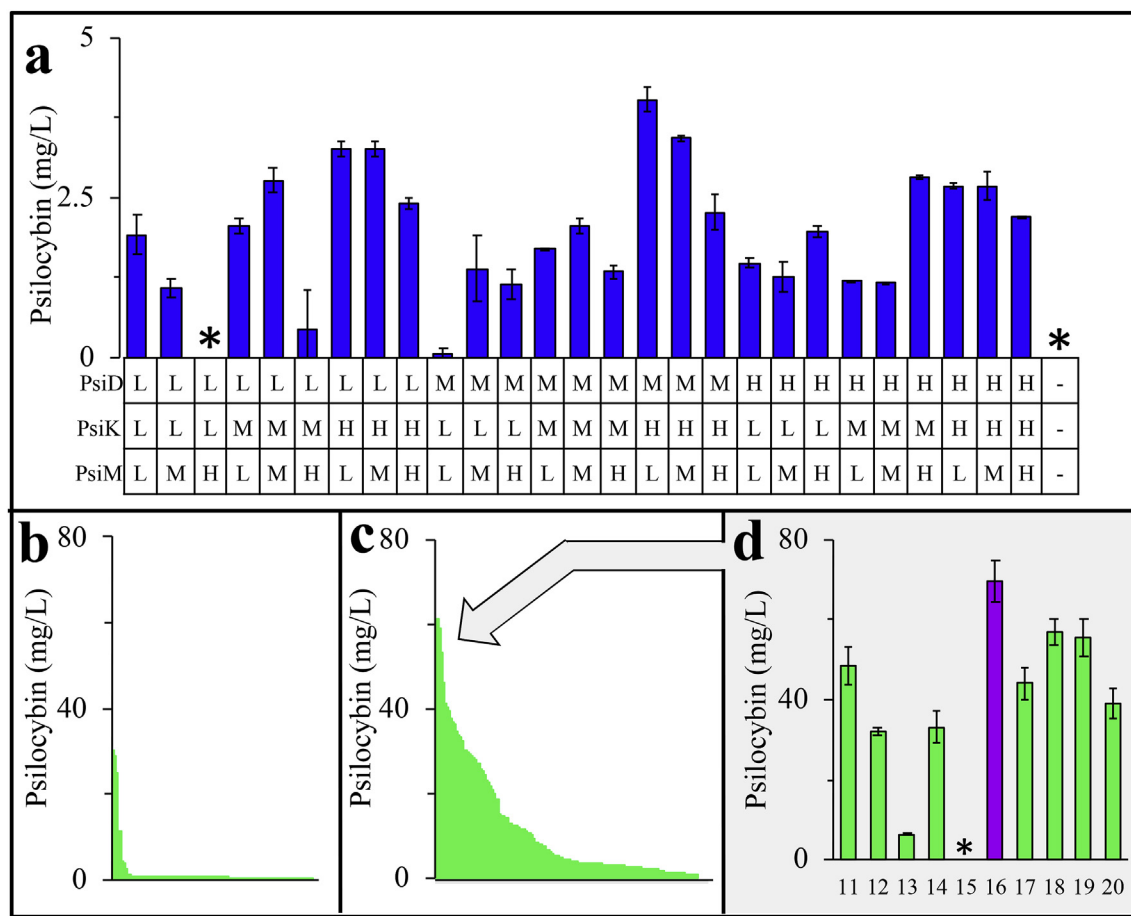
Fig. 2. Summary of genetic optimization strategies. (a) Defined copy number library screening. The biosynthetic genes *psiD*, *psiK*, and *psiM* were expressed at either a high (H), medium (M), or low (L) copy number as indicated above. (b) Pseudooperon library screening. The library provided very few mutant constructs with enhanced ability to produce psilocybin over levels previously achieved in the defined copy number library. (c) Basic operon library screening. Significant enhancement of library performance was observed over the pseudooperon library. (d) Additional screening of top mutants from operon library. The top 10 mutants from the operon library study were subjected to recloning and rescreening under standard conditions. Operon library clones #13 and #15 (Fig. 2d) demonstrated a large reduction in product titer and were identified as false positives in the original screen. Operon clone #16 (pPsilo16, purple) was selected for further study. All combinations were screened in 48-well plates under standard screening conditions and quantified using HPLC analysis. Error bars represent ± 1 standard deviation from the mean of replicate samples. *Psilocybin not detected. (For interpretation of the references to color in this figure legend, the reader is referred to the Web version of this article.)

S4–S6).

2.2. Defined copy number library

A defined 27-member copy number library consisting of the 3 heterologous biosynthesis genes (*psiD*, *psiK*, and *psiM*) each expressed on 3 different copy number plasmids was constructed and screened in 48-well plates as shown in Fig. 2a. Each member of the library contained each of the three genes spread across a low (pACM4-SDM2x), medium (pCDM4-SDM2x), or high (pETM6-SDM2x) copy number plasmid (Fig. 1a). The functional expression levels (low, medium, high) for this set of plasmid expression vectors has been previously reported in the literature (Xu et al., 2013a, 2012). This library screen realized minor improvements over the original All-High construct (2.19 ± 0.02 mg/ L), where final titers of 4.0 ± 0.2 mg/L were achieved with the combination of psiK expressed from the pETM6-SDM2x vector, psiD expressed from the pCDM4-SDM2x vector, and psiM expressed from the pACM4-SDM2x vector in the BL21 star™ (DE3) expression host.

2.3. Pseudooperon library

The pseudooperon library constructs have a different mutant promoter in front of each of the three enzyme encoding sequences, *psiD*,

psiK, and *psiM*, while having a single terminator at the end of the 3-gene synthetic operon (Fig. 1b). This configuration results in a widely variable transcriptional landscape in which each promoter results in a distinct mRNA capable of encoding translation of either 1, 2, or 3 of the pathway enzymes. In this configuration, a possible library size of 125 pathway configurations exist, and 231 random colonies were screened. The large majority of variants demonstrated low (30%) or no production (65%, data not shown); however, a small population of mutants demonstrated significant improvements in production (Fig. 2b) over the previous defined library screen (Fig. 2a). Additional analysis of the HPLC data revealed a significant accumulation of the intermediate, 4-hydroxytryptophan, suggesting that poor functional activity from the PsiD enzyme led to the underperformance of the majority of the members in the pseudooperon library (Fig. S5).

2.4. Basic operon library

In the operon configuration, the three-gene pathway was expressed from a single high-copy plasmid under the control of a single promoter and terminator where each gene has an identical ribosome binding site (RBS) (Fig. 1c). The promoter sequence was randomized to one of five mutant T7 promoters (G6, H9, H10, C4, Consensus) using the ePathOptimize approach (Jones et al., 2015a,b), resulting in a library that

contains 5 potential promoter combinations (Fig. 2c). After screening nearly 50× the library size, the top 10 variants were selected for further screening. These top variants were re-cloned into an empty plasmid backbone and transformed to eliminate the possibility of spurious plasmid or strain mutations (Fig. 2d). Mutant #16 (pPsilo16) was selected for further investigation due to its top production and high reproducibility across multiple fermentations. The sequencing results revealed that pPsilo16 contains the H10 mutant promoter which has been previously characterized as a medium strength promoter, with between 40% and 70% of the effective expression strength of the consensus T7 sequence (Jones et al., 2015a, b). The top mutants from the basic operon screen show a 17-fold improvement in titer over the best performing mutants from the defined copy number library study.

2.5. Fermentation conditions optimization

After identifying pPsilo16 as the best strain with respect to highest psilocybin production, low buildup of intermediate products, and consistent reproducibility, the strain underwent a series of optimization experiments to determine the best fermentation conditions for the production of psilocybin. All genetic optimization experiments were conducted under standard conditions (as described in the methods) determined from initial screening in our earlier proof-of-principle studies (data not shown). Many studies in the metabolic engineering literature have demonstrated high sensitivity to variations in induction point for pathways controlled by the T7-*lac* inducible promoter (Hannig and Makrides, 1998; Jones and Koffas, 2016; Studier, 2005). Additionally, induction timing can have a large impact on overall cell growth and can lead to difficulties achieving reproducible production upon scale-up (Jones et al., 2015a, b; Wu et al., 2016). Upon evaluation of induction sensitivity for pPsilo16, we found that the cells demonstrate low sensitivity to induction point, with the maximum production achieved with induction 3–4 h post inoculation (Fig. 3a). No psilocybin production was observed in the non-induced controls (data not shown).

Next, optimization of base media selection, carbon source identity, and inducer concentration was evaluated. Since these variables can affect cellular growth rate and corresponding optimal induction points, each of these variables were evaluated across a range of induction points from 1 to 6 h (Figs. S8–S10). As demonstrated in Fig. 3b, psilocybin production was very sensitive to both media and carbon source selection ($p < 0.05$). When production was attempted in a rich undefined media such as LB, a dark colored insoluble product was observed along with low psilocybin production. Similarly, low production was also observed when grown on glycerol, however no colored products were observed. pPsilo16 demonstrated moderate sensitivity to IPTG concentration, with higher final concentrations of 0.5 and 1.0 mM outperforming 0.1 mM over a range of induction time conditions ($p < 0.05$) (Fig. 3b). This trend is likely influenced by the initial library screening, which was performed at 1.0 mM IPTG.

Production temperatures of 30, 37, 40, and 42 °C were also evaluated for their effect on psilocybin production (Fig. 3a). In an attempt to minimize the effect on changing optimal induction points, all fermentations were started at 37 °C through the growth phase of the fermentation before being shifted to the production temperature 1 h prior to induction. A significant preference ($p < 0.05$) was seen for maintaining an isothermal fermentation temperature of 37 °C throughout both growth and production phases (Fig. 3a).

The fermentation optimization was completed by evaluating the effects of the targeted media supplements: 4-hydroxyindole, serine, and methionine (Fig. 3c). Each media supplement was provided at high, medium, and low levels: 4-hydroxyindole (150, 350, and 500 mg/L), serine and methionine (0, 1, and 5 g/L). At high concentrations of 4-hydroxyindole, the cells demonstrated noticeable growth decline due to presumed cellular toxicity leading to reduced productivity. Serine addition showed minimal effects on psilocybin production, however, the addition of methionine in the presence of greater than 350 mg/L of 4-

hydroxyindole resulted in a significant enhancement of psilocybin titer ($p < 0.05$). Under the identified optimal screening conditions, psilocybin was produced at 139 ± 2.7 mg/L, which represents a 63-fold improvement through the synergistic efforts of genetic and fermentation optimization.

2.6. Scale-up study

After identification of optimized production conditions for pPsilo16, a fed-batch scale up study was completed as described in the methods. This study resulted in the production of 1.16 g/L of psilocybin which represents an 8.3-fold improvement over the top conditions optimization screening case in 48-well plates and a 528-fold improvement over the original unoptimized construct. Precursor and intermediate product titers remained low throughout the fermentation enabling the culture to achieve a final OD_{600} of 35 (Fig. 4b). Pathway intermediate concentrations were maintained at a low level through the use of a HPLC informed feeding strategy which enabled the substrate feed rate to be tailored to specific pathway bottleneck flux within 45 min of sampling. This led to an oscillatory concentration profile for the key pathway intermediate 4-hydroxytryptophan (Fig. 4b). The initial 20 g/L of glucose was completely consumed from the media after 25 h and was then externally fed such that the culture maintained robust growth with low residual sugar content in the media to maximize product yield on glucose.

3. Discussion and conclusion

This work shows the first reported case of *in vivo* psilocybin production using a prokaryotic host. Furthermore, this work highlights the power of tandem genetic and fermentation optimization to quickly identify key process parameters required to enable successful scale-up studies culminating in gram scale production of a high-value chemical product.

In the initial proof-of-principle study, the production of psilocybin and all pathway intermediates were confirmed through the use of high mass accuracy LC-MS (Fig. S3). HPLC analysis of fermentation broth from strains containing incomplete pathways (i.e. psiDM and psiDK) was consistent with the conclusions of previous studies (Fricke et al., 2017) aimed at identifying the order of specific biosynthetic steps in the synthesis pathway (data not shown).

Multiple genetic optimization methods were utilized in parallel to identify a genetically superior mutant. Starting with the copy number-based approach, we constructed a 27-member library of 3 pathway genes, each at 3 discrete copy numbers (Fig. 2a). Of the three genetic optimization screens presented, this method was the most tedious to construct, requiring each plasmid to be independently cloned and verified prior to screening. This defined library approach also yielded the lowest product titers with the best mutants demonstrating small but statistically significant ($p < 0.05$) improvements over the All-High initial construct. Although a similar modular optimization approach has previously proven successful for a range of products including taxadiene (Ajikumar et al., 2010), free fatty acids (Xu et al., 2013b), and others (Biggs et al., 2014; Juminaga et al., 2012; Wu et al., 2013b). We suspect the limited titer improvement from this approach is likely due to the increased metabolic burden associated with selection for and propagation of three independent plasmids (Wu et al., 2016).

Subsequent screening of two independent single-plasmid transcriptionally-varied promoter libraries with pathway genes in basic operon (Fig. 2c) and pseudooperon (Fig. 2b) configuration yielded considerably improved results over the initial copy number library. In each case, the library was screened using a medium-throughput HPLC-based screen. Each of these transcriptionally varied libraries were constructed using the high copy pETM6 plasmid vector. This enabled a wide range of expression levels to be screened, resulting in greater coverage of the psilocybin transcriptional landscape. The pseudooperon
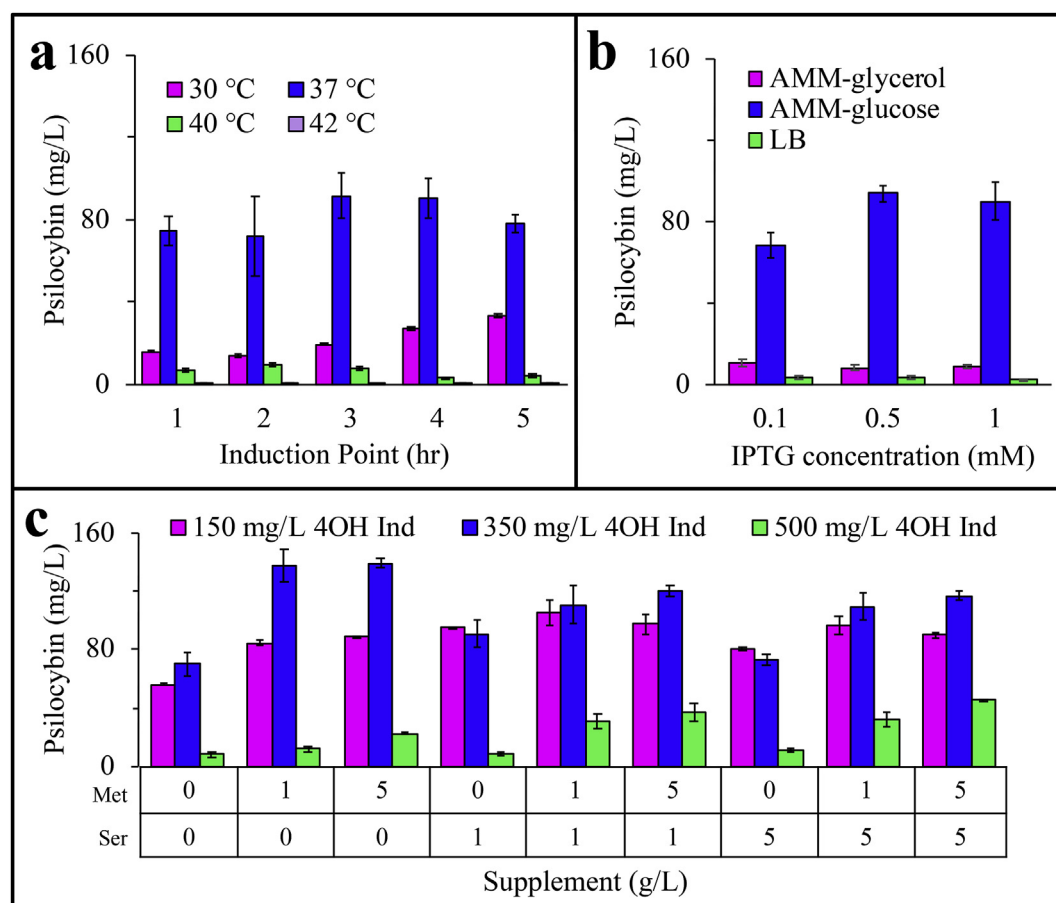
Fig. 3. Summary of fermentation conditions optimization studies. (a) Induction point and temperature optimization. The timing of IPTG induction was varied from 1 to 5 h post inoculation. The data suggest reduced sensitivity to induction point but high sensitivity to production phase temperature with optimal production occurring at 37 °C. (b) Media, carbon source, and inducer concentration screening. A significant preference was shown for AMM with glucose as the carbon source. (c) Effects of media supplementation on psilocybin titer. High sensitivity was observed for changes in the supplement concentration for 4-hydroxyindole, serine, and methionine. Error bars represent ± 1 standard deviation from the mean of replicate samples.
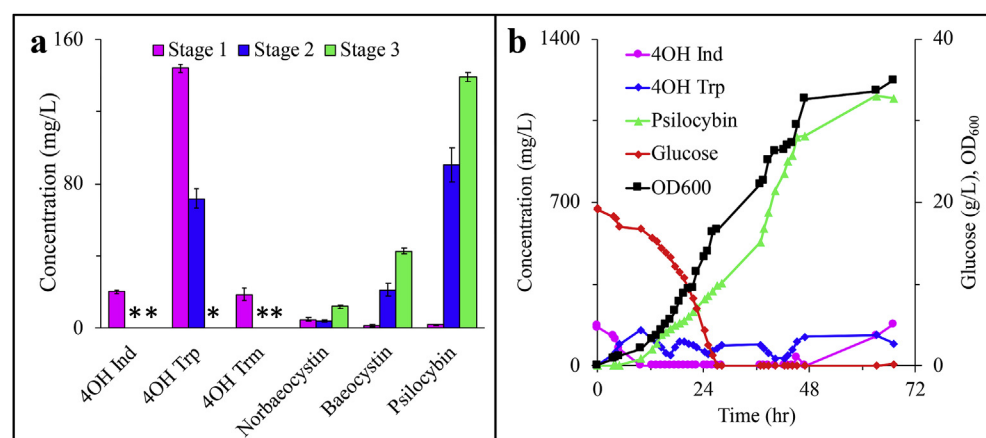

Fig. 4. Optimization evaluation and bioreactor scale up. (a) Comparison of intermediate and final product titers at various stages of optimization. Stage 1 – Initial proof-of-concept All-High control, Stage 2 – pPsilo16 post genetic optimization, Stage 3 – pPsilo16 post genetic and fermentation optimization. Each additional optimization stage further improved final product titer through reduction of intermediate product buildup. 4OH Ind: 4-hydroxyndole, 4OH-Trp: 4-hydroxytryptophan, 4OH Trm: 4-hydroxytryptamine. (b) Fed-batch bioreactor scale up. Through careful monitoring of 4-hydroxyindole feed rate, the concentration of all intermediate products could be kept low resulting in improved growth and psilocybin titers. Error bars represent ± 1 standard deviation from the mean of replicate samples. *compound not detected.

library screen demonstrated that a large majority of mutants (~95%) showed low or no psilocybin production. The reason for this widespread underperformance is unknown; however, it does motivate the use of random libraries coupled with variant screening for the identification of genetically superior mutants as the current predictive power of *a priori* pathway design is still lacking for most applications. Surprisingly, the simplistic basic-operon pathway design yielded the highest titer

psilocybin production in this study. This coupled with the smallest library size of only 5 mutants, enabled rapid screening of several times the theoretical library size, resulting in high confidence of complete coverage of the full transcriptional landscape. Upon recloning and re-screening the top mutants from the operon library screen, several false positives were identified as shown in Fig. 2d. The source of error for these false positive mutants was not investigated as the false positive

rate was at an acceptable level for the study design.

Additional increases in titer and yield were achieved through careful optimization of fermentation conditions (Fig. 3). The genetically superior strain, pPsilo16, demonstrated low sensitivity to induction timing as compared to that of other amino acid derived high-value products (Ahmadi and Pfeifer, 2016; Jones et al., 2015a, b; Jones et al., 2016; Wu et al., 2013a); however, this could also be due to the supplementation of both 4-hydroxyindole and serine to the fermentation media, reducing the requirement for high flux through amino acid metabolism. Therefore, all additional fermentation optimization experiments were performed under a range of induction times. Little variation from the induction optimum of 4 h post inoculation was observed, strengthening the observation of reduced sensitivity to induction timing.

The psilocybin production host demonstrated high sensitivity to media composition, carbon source identity, fermentation temperature, and inducer concentration (Fig 3a and b). In each case, this preferred level was similar to that of the standard screening conditions. This is likely not a coincidence, as some basic initial screening was performed to identify conditions under which our proof-of-principle strain best performed. Furthermore, the initial genetic screening studies were performed under standard screening conditions, which also self-selects for mutants with top performance under the test conditions.

The largest gains in the fermentation optimization aspect of this study were achieved through the media supplementation studies (Fig. 3c). In this study, the concentrations of 4-hydroxyindole, serine, and methionine were varied. These supplements were selected specifically for their direct effect on the psilocybin production pathway (Fig. 1d). 4-hydroxyindole and serine are condensed by TrpAB in the first dedicated step of the pathway to form the intermediate 4-hydroxytryptophan. Although E. coli can produce serine and indole naturally, it lacks the ability to express the P450 hydroxylase that oxidizes indole into 4-hydroxyindole. Additionally, with the high fluxes through our engineered pathway, we hypothesized that the cellular supply of serine would be quickly depleted, requiring additional supplementation to not limit pathway flux. Finally, methionine was supplemented to enhance intercellular pools of the activated methyl donor, SAM. The final two biosynthetic steps are both catalyzed by the SAM-dependent methyltransferase, PsiM. Previous studies with SAM-dependent methylations in E. coli have documented SAM-limited flux to final products (Cress et al., 2017; Kunjapur et al., 2016). In each of these cases, the need for the media supplementation can be addressed using metabolic engineering approaches that are beyond the scope of this study, but certainly applicable in future studies to improve the efficiency of psilocybin production in vivo.

Analysis of intermediate product concentrations was performed to evaluate the success of each optimization study. A comparison is presented (Fig. 4a) between the initial proof-of-principle 'All-High' strain (Stage 1) and the top production strain, both post genetic optimization (Stage 2) and post genetic and fermentation optimization (Stage 3). Each additional optimization stage resulted in further enhanced psilocybin titers, accomplished through a reduction in intermediate product concentrations, and generally enhanced flux towards the final product.

The information gained from the genetic and fermentation optimization studies was applied in a scale-up study for the production of psilocybin in a fed-batch bioreactor. In this study, many of the optimization parameters such as temperature, inducer concentration, and induction timing were applied as previously optimized. Information from the supplement addition studies was used but applied with modification from the 2 mL batch studies. In the fed-batch studies, both serine and methionine were supplemented at the high level of 5 g/L to account for higher cellular demand due to enhanced cell growth. Furthermore, in the small-scale studies a growth deficit was observed at higher concentrations of 4-hydroxyindole and 4-hydroxytryptophan. To counter this, a low amount of 4-hydroxyindole (150 mg/L) was added initially to the media, while a low-flow syringe pump, containing a 40 mg/mL 4-hydroxyindole solution, was connected for slow external supplementation. To determine the optimal feed rate, the pathway flux through the bottleneck point, PsiD, was estimated through frequent HPLC analysis of the fermentation broth. As 4-hydroxytryptophan titers fell, the flux of 4-hydroxyindole was increased to meet the high flux demand, and vise-versa. This strategy resulted in an oscillatory concentration profile for 4-hydroxytryptophan and maintained all intermediates at low levels, enabling robust and extended growth and psilocybin production (Fig. 4b). Additional details on substrate feed rate, cumulative yield, and bioreactor parameters (agitation, DO, pH, and temperature) can be found in Supplementary Figure 11.

In small batch fermentation studies, the work presented above resulted in a similar titer of psilocybin to that presented previously in the A. nidulans host (Hoefgen et al., 2018). This indicates that both bacterial and fungal hosts show potential as production platforms for this important chemical. However, upon scale-up to a fed batch reactor our bacterial host demonstrated greatly enhanced psilocybin production resulting in a 10-fold enhancement over previously published results.

In conclusion, we have presented the first example of psilocybin production in a prokaryotic organism and the highest psilocybin titer to date from a recombinant host from any kingdom. This was accomplished through the combination of genetic and fermentation optimization in small scale, coupled with a scaled-up fed-batch study utilizing a unique HPLC informed substrate feeding strategy. The fed-batch study resulted in a psilocybin titer of 1.16 g/L with maximum and final molar yields from the 4-hydroxyindole substrate of 0.60 and 0.38 mol/mol, respectively (Fig. S11d). Future efforts to enhance the strain background to enable de novo production of psilocybin, without the need for chemical supplementation, could enable a biologically synthesized psilocybin pharmaceutical product to compete with chemical synthesis strategies for applications in medicine, psychology, and neurobiology.

4. Methods

4.1. Bacterial strains, vectors, and media

E. coli DH5α was used to propagate all plasmids, while BL21 star™ (DE3) was used as the host for all chemical production experiments. Plasmid transformations were completed using standard electro and chemical competency protocols as specified. Unless noted otherwise, Andrew's Magic Media (AMM) (He et al., 2015) was used for both overnight growth and production media, while Luria Broth (LB) was used for plasmid propagation during cloning. The antibiotics ampicillin (80 μg/mL), chloramphenicol (25 μg/mL), and streptomycin (50 μg/mL) were added at their respective concentrations to the culture media when using pETM6, pACM4, and pCDM4-derived vectors, respectively. A description of all plasmids and strains used in this study can be found in Table S1. The exogenous pathway genes encoding the enzymes PsiD, PsiK, and PsiM contained on plasmids pJF24, pJF23, and pFB13, respectively, were a generous gift from the Hoffmeister group (Fricke et al., 2017).

4.2. Plasmid construction

The original ePathBrick expression vectors, #4, #5, and #6 (Table S1) were modified through two rounds of site directed mutagenesis with primers 1 through 4 (Table S2) to result in the corresponding 'SDM2x' series of vectors: #7, #8, and #9 (Table S1). This mutagenesis was performed to swap the positions of the isocaudomer restriction enzyme pair XmaJI/XbaI in the vector. This change allows for the monocistronic and pseudooperon pathway configurations to be constructed more cost efficiently by avoiding the use of the costly XmaJI restriction enzyme. This series of vectors was then used to construct the vectors used in the defined copy number library study #10 - #27 (Table S1).

Plasmids #1 - #3 containing psiD, psiK, and psiM, respectively,

were restriction enzyme digested with *Nde*I and *Hind*III, gel extracted, and ligated into the pETM6-SDM2x (#7, Table S1) plasmid backbone, resulting in plasmids #10, #11, and #12 (Table S1). All multigene expression plasmids were constructed in pseudooperon configuration using a modified version of the previously published ePathBrick methods as described above, while all transcriptional libraries were constructed using standard ePathOptimize methods (Jones et al., 2015a, b; Xu et al., 2012).

4.3. Standard screening conditions

Standard screening was performed in 2 mL working volume cultures in 48-well plates at 37 °C. AMM supplemented with serine (1 g/L), 4-hydroxyindole (350 mg/L), and appropriate antibiotics were used unless otherwise noted. Overnight cultures were grown from either an agar plate or freezer stock culture in AMM with appropriate antibiotics and supplements for 14–16 h in a shaking 37 °C incubator. Induction with 1 mM isopropyl β-D-1-thiogalactopyranoside (IPTG) occurred 4 h after inoculation, unless otherwise noted. Cultures were then sampled 24 h post inoculation and subjected to HPLC analysis as described in analytical methods below.

4.4. Library construction

The defined copy number library was constructed using plasmid #7 (High), #8 (Medium), and #9 (Low). The pathway genes were modulated in either the high, medium, and low copy number vectors, as shown in Fig. 2a. The BL21 star™ (DE3) production host was transformed with the appropriate plasmids such that each strain had all three vectors, even if some were empty, to enable the same antibiotic resistance burden to be present in all defined library members (Fig. 1a). In the cases where multiple genes were present at a single expression level, the plasmids were constructed in pseudooperon configuration as described above.

Random promoter libraries were assembled using standard ePathOptimize methods with the five original mutant T7 promoters: G6, H9, H10, C4, and consensus. Random libraries were built in pseudooperon (Fig. 1b) and basic operon (Fig. 1c) forms, maintaining a sufficient number of colonies at each cloning step as to not limit library size.

4.5. Fermentation optimization

Once a genetically superior production strain, pSilo16 (#28, Table S1) was identified, fermentation conditions were optimized to further enhance psilocybin production. The effect of varying induction timing was first investigated under standard screening conditions, then further evaluated under other conditions that have been shown to affect cellular growth rate and subsequently optimal induction timing including: 1. base media identity (AMM, LB), 2. media carbon source (glucose, glycerol), 3. production temperature (30 °C, 37 °C, 40 °C, 42 °C), 4. inducer concentration (1 mM, 0.5 mM, 0.1 mM), 5. concentration of media supplements: serine and methionine (0 g/L, 1 g/L, 5 g/L), and 6. concentration of 4-hydroxyindole substrate (150 mg/L, 350 mg/L, 500 mg/L). All screening was completed in 48-well plates under standard screening conditions unless otherwise noted.

4.6. Scale-up study

In order to demonstrate the scalability of our optimized production host and process, a scale-up study was performed in an Eppendorf BioFlo120 bioreactor with 1.5 L working volume. The cylindrical vessel was mixed by a direct drive shaft containing two Rushton-type impellers positioned equidistance under the liquid surface. The overnight culture of Psilo16 was grown for 14 h at 37 °C in AMM supplemented with serine (5 g/L), methionine (5 g/L), and appropriate antibiotics.

The bioreactor was inoculated at 2% v/v to an initial OD_{600} of approximately 0.09. The bioreactor was initially filled with AMM media (1.5 L) supplemented with 150 mg/L 4-hydroxyindole, 5 g/L serine, and 5 g/L methionine. Temperature was held constant at 37 °C with a heat jacket and recirculating cooling water, pH was automatically controlled at 6.5 with the addition of 10 M NaOH, and dissolved oxygen (DO) was maintained at 20% of saturation through agitation cascade control (250–1000 rpm). Full oxygen saturation was defined under the conditions of 37 °C, pH 7.0, 250 rpm agitation, and 3 lpm of standard air. The zero-oxygen set point was achieved by a nitrogen gas flush. Samples were collected periodically for measurement of OD_{600} and metabolite analysis. The bioreactor was induced with 1 mM IPTG 4 h post inoculation. Once the initial 20 g/L of glucose was exhausted, as identified by a DO spike, separate feed streams of 500 g/L glucose and 90 g/L $(NH_4)_2HPO_4$ were fed at a flow rate ranging from 2.0 to 4.0 mL/L/hr (Fig. S11b). Beginning 12 h post inoculation, a continuous supply of 4-hydroxyindole was supplied by external syringe pump to the bioreactor. The feed rate of 4-hydroxyindole was manually varied from 11 to 53 mg/L/hr according to the observed buildup of the key pathway intermediate 4-hydroxytryptophan (Fig. S11c). The concentration of psilocybin and all intermediate compounds were immediately analyzed via HPLC on an approximate 45-min delay and were used as feedback into the feeding strategy described above.

4.7. Analytical methods

Samples were prepared by adding an equal volume of 100% ethanol or 100% deionized water and fermentation broth, vortexed briefly, and then centrifuged at $12,000 \times g$ for 10 min 2 µL of the resulting supernatant was then injected for HPLC or LC-MS analysis. Analysis was performed on a Thermo Scientific Ultimate 3000 High-Performance Liquid Chromatography (HPLC) system equipped with Diode Array Detector (DAD) and Refractive Index Detector (RID). Authentic standards were purchased for glucose (Sigma), psilocybin (Cerilliant), and 4-hydroxyindole (BioSynth). Standards for baeocystin, norbaeocystin, 4-hydroxytryptamine, and 4-hydroxytryptophan were quantified using a standard for a similar analog due to limited commercial availability and extremely high cost, approx. $2000 USD for 1 mg of the authentic standard. Baeocystin and norbaeocystin were quantified on the psilocybin standard curve, while 4-hydroxytryptamine and 4-hydroxytryptophan were quantified on the standard curves of 5-hydroxytryptamine (Alfa Aesar) and 5-hydroxytryptophan (Alfa Aesar), respectively (Fig. S1). No significant intracellular accumulation of target metabolites was observed upon analysis with and without cell lysis. Transport across the cell membrane was assumed to be passive, however, specific investigation into this phenomenon was not undertaken for this work.

Glucose analysis was performed using an Aminex HPX-87H column maintained at 30 °C followed by a refractive index detector (RID) held at 35 °C. The mobile phase was 5 mM H_2SO_4 in water at a flow rate of 0.6 mL/min. Glucose was quantified using a standard curve with a retention time of 8.8 min.

UV absorbance at 280 nm was used to quantify all aromatic compounds. Analysis was performed using an Agilent ZORBAX Eclipse XDB-C18 analytical column (3.0 mm × 250 mm, 5 µm) with mobile phases of acetonitrile (A) and water (B) both containing 0.1% formic acid at a flow rate of 1 mL/min: 0 min, 5% A; 0.43 min, 5% A; 5.15 min, 19% A; 6.44 min, 100% A; 7.73 min 100% A; 7.73 min, 5% A; 9.87 min, 5% A. This method resulted in the following observed retention times: psilocybin (2.2 min), baeocystin (1.7 min), norbaeocystin (1.9 min), 4-hydroxytryptamine (3.4 min), 4-hydroxytryptophan (3.6 min), and 4-hydroxyindole (6.6 min). High Resolution Liquid Chromatography Mass Spectrometry (LC-MS) and Mass Spectrometry-Mass Spectrometry (LC-MS/MS) data were measured on a Thermo Scientific LTQ Orbitrap XL mass spectrometer equipped with an Ion Max ESI source using the same mobile phases and column described above. The flow rate was adjusted

to 0.250 mL/min resulting in a method with the following gradient: 0 min, 5% A; 1 min, 5% A; 24 min, 19% A; 30 min, 100% A; 36 min 100% A; 36 min, 5% A; 46 min, 5% A. This method resulted in the following observed retention times: psilocybin (8.7 min), baeocystin (7.6 min), norbaeocystin (6.4 min), 4-hydroxytryptamine (13.3 min), 4-hydroxytryptophan (14.2 min), and 4-hydroxyindole (27 min). The Orbitrap was operated in positive mode using direct infusion from a syringe at 5 μl/min for optimization of tuning parameters and for external calibration. A 5-hydroxytryptamine sample was prepared at ~0.1 mg/ml (570 μM) in 50% ethanol/50% water for tuning. External calibration was performed using the Pierce LTQ ESI Positive Ion Calibration Solution, allowing for a less than 5 ppm mass accuracy.

Mass spectrometry parameters in positive mode were spray voltage 3.5 kV, capillary temperature 275 °C, capillary voltage 23 V and tube lens voltage 80 V (optimized by tuning on 5-hydroxytryptamine), nitrogen sheath, auxiliary, and sweep gas were 15, 30, 1 a. u., full scan mode (m/z 100–500) at a resolution of 60,000 and an AGC target of 1e6.

LC-MS/MS data was collected in the data-dependent acquisition mode, where the full MS scan was followed by fragmentation of the three most abundant peaks by higher energy collisional dissociation (HCD). Data was collected in the Orbitrap with a minimum m/z of 50 at 30,000 resolution, AGC target of 1e5, and intensity threshold of 200 K using normalized collision energy of 40, default charge state of 1, activation time of 30 ms, and maximum injection times of 200 msec for both MS and MS/MS scans. All data were processed using Xcalibur/Qual Browser 2.1.0 SP1 build (Thermo Scientific). MS/MS fragmentation data can be found in the supplementary materials (Fig. S3).

Appendix A. Supplementary data

Supplementary data to this article can be found online at https://doi.org/10.1016/j.ymben.2019.09.009.

Contributions

A.M.A., N.A.K., Z.W., and J.A.J. designed experiments. A.M.A., N.A.K., Z.W., J.D.B., C.S.M., A.L.E., and J.A.J. performed experiments. T.A.R. performed LC-MS analysis. A.M.A., T.A.R., and J.A.J. analyzed data and wrote the manuscript. All authors reviewed and edited the manuscript.

Conflicts of interest

The authors declare no conflicts of interest.

References

Ahmadi, M.K., Pfeifer, B.A., 2016. Recent progress in therapeutic natural product biosynthesis using *Escherichia coli*. Curr. Opin. Biotechnol. 42, 7–12. https://doi.org/10.1016/j.copbio.2016.02.010.

Ajikumar, P.K., Xiao, W.-H., Tyo, K.E.J., Wang, Y., Simeon, F., Leonard, E., Mucha, O., Phon, T.H., Pfeifer, B., Stephanopoulos, G., 2010. Isoprenoid pathway optimization for Taxol precursor overproduction in *Escherichia coli*. Science 330, 70–74. https://doi.org/10.1126/science.1191652.

Belser, A.B., Agin-Liebes, G., Swift, T.C., Terrana, S., Devenot, N., Friedman, H.L., Guss, J., Bossis, A., Ross, S., 2017. Patient experiences of psilocybin-assisted psychotherapy: an interpretative phenomenological analysis. J. Humanist. Psychol. 57, 354–388. https://doi.org/10.1177/0022167817706884.

Biggs, B.W., De Paepe, B., Santos, C.N.S., De Mey, M., Kumaran Ajikumar, P., 2014. Multivariate modular metabolic engineering for pathway and strain optimization. Curr. Opin. Biotechnol. 29, 156–162. https://doi.org/10.1016/j.copbio.2014.05.005.

Blei, F., Baldeweg, F., Fricke, J., Hoffmeister, D., 2018. Biocatalytic production of psilocybin and derivatives in tryptophan synthase-enhanced reactions. Chem. Eur J. 24, 10028–10031. https://doi.org/10.1002/chem.201801047.

Buller, A.R., Brinkmann-Chen, S., Romney, D.K., Herger, M., Murciano-Calles, J., Arnold, F.H., 2015. Directed evolution of the tryptophan synthase β-subunit for stand-alone function recapitulates allosteric activation. Proc. Natl. Acad. Sci. U.S.A 112, 14599–14604. https://doi.org/10.1073/pnas.1516401112.

Carhart-Harris, R.L., Bolstridge, M., Rucker, J., Day, C.M.J., Erritzoe, D., Kaelen, M., Bloomfield, M., Rickard, J.A., Forbes, B., Feilding, A., Taylor, D., Pilling, S., Curran, V.H., Nutt, D.J., 2016. Psilocybin with psychological support for treatment-resistant depression: an open-label feasibility study. The Lancet Psychiatr. 3, 619–627. https://doi.org/10.1016/S2215-0366(16)30065-7.

Carhart-Harris, R.L., Roseman, L., Bolstridge, M., Demetriou, L., Pannekoek, J.N., Wall, M.B., Tanner, M., Kaelen, M., McGonigle, J., Murphy, K., Leech, R., Curran, H.V., Nutt, D.J., 2017. Psilocybin for treatment-resistant depression: fMRI-measured brain mechanisms. Sci. Rep. 7, 13187. https://doi.org/10.1038/s41598-017-13282-7.

Cress, B.F., Leitz, Q.D., Kim, D.C., Amore, T.D., Suzuki, J.Y., Linhardt, R.J., Koffas, M.A.G., 2017. CRISPRi-mediated metabolic engineering of *E. coli* for O-methylated anthocyanin production. Microb. Cell Factories 16, 10. https://doi.org/10.1186/s12934-016-0623-3.

Fricke, J., Blei, F., Hoffmeister, D., 2017. Enzymatic synthesis of psilocybin. Angew. Chem. Int. Ed. 56, 12352–12355. https://doi.org/10.1002/anie.201705489.

Fricke, J., Lenz, C., Wick, J., Blei, F., Hoffmeister, D., 2019. Production options for psilocybin: making of the magic. Chem. Eur J. 25, 897–903. https://doi.org/10.1002/chem.201802758.

Gluff, J.A., Teolis, M.G., Moore, A.A., Kelly, D.R., 2017. Post-traumatic stress disorder (PTSD): a webliography. J. Consum. Health Internet 21, 389–401. https://doi.org/10.1080/15398285.2017.1377539.

Grob, C.S., Danforth, A.L., Chopra, G.S., Hagerty, M., McKay, C.R., Halberstadt, A.L., Greer, G.R., 2011. Pilot study of psilocybin treatment for anxiety in patients with advanced-stage cancer. Arch. Gen. Psychiatr. 68, 71. https://doi.org/10.1001/archgenpsychiatry.2010.116.

Hannig, G., Makrides, S.C., 1998. Strategies for optimizing heterologous protein expression in *Escherichia coli*. Trends Biotechnol. 16, 54–60. https://doi.org/10.1016/S0167-7799(97)01155-4.

He, W., Fu, L., Li, G., Andrew Jones, J., Linhardt, R.J., Koffas, M., 2015. Production of chondroitin in metabolically engineered *E. coli*. Metab. Eng. 27, 92–100. https://doi.org/10.1016/J.YMBEN.2014.11.003.

Hoefgen, S., Lin, J., Fricke, J., Stroe, M.C., Mattern, D.J., Kufs, J.E., Hortschansky, P., Brakhage, A.A., Hoffmeister, D., Valiante, V., 2018. Facile assembly and fluorescence-based screening method for heterologous expression of biosynthetic pathways in fungi. Metab. Eng. 48, 44–51. https://doi.org/10.1016/J.YMBEN.2018.05.014.

Hofmann, A., Frey, A., Ott, H., Petr zilka, T., Troxler, F., 1958. Elucidation of the structure and the synthesis of psilocybin. Experientia 14, 397–399. https://doi.org/10.1007/BF02160424.

Hofmann, A., Heim, R., Brack, A., Kobel, H., Frey, A., Ott, H., Petrzilka, T., Troxler, F., 1959. Psilocybin und psilocin, zwei psychotrope wirkstoffe aus mexikanischen rauschpilzen. Helv. Chim. Acta 42, 1557–1572. https://doi.org/10.1002/hlca.19590420518.

Johnson, M.W., Griffiths, R.R., 2017. Potential therapeutic effects of psilocybin. Neurotherapeutics 14, 734–740. https://doi.org/10.1007/s13311-017-0542-y.

Johnson, M.W., Griffiths, R.R., Hendricks, P.S., Henningfield, J.E., 2018. The abuse potential of medical psilocybin according to the 8 factors of the Controlled Substances Act. Neuropharmacology 142, 143–166. https://doi.org/10.1016/j.neuropharm.2018.05.012.

Jones, J.A., Koffas, M.A.G., 2016. Optimizing metabolic pathways for the improved production of natural products. Methods Enzymol. 575, 179–193. https://doi.org/10.1016/BS.MIE.2016.02.010.

Jones, J Andrew, Toparlak, Ö.D., Koffas, M.A., 2015a. Metabolic pathway balancing and its role in the production of biofuels and chemicals. Curr. Opin. Biotechnol. 33, 52–59. https://doi.org/10.1016/j.copbio.2014.11.013.

Jones, J. Andrew, Vernacchio, V.R., Lachance, D.M., Lebovich, M., Fu, L., Shirke, A.N., Schultz, V.L., Cress, B., Linhardt, R.J., Koffas, M.A.G., 2015b. ePathOptimize: a combinatorial approach for transcriptional balancing of metabolic pathways. Sci. Rep. 5, 11301. https://doi.org/10.1038/srep11301.

Jones, J.A., Vernacchio, V.R., Sinkoe, A.L., Collins, S.M., Ibrahim, M.H.A., Lachance, D.M., Hahn, J., Koffas, M.A.G., 2016. Experimental and computational optimization of an *Escherichia coli* co-culture for the efficient production of flavonoids. Metab. Eng. 35, 55–63. https://doi.org/10.1016/J.YMBEN.2016.01.006.

Juminaga, D., Baidoo, E.E.K., Redding-Johanson, A.M., Batth, T.S., Burd, H., Mukhopadhyay, A., Petzold, C.J., Keasling, J.D., 2012. Modular engineering of l-Tyrosine production in *Escherichia coli*. Appl. Environ. Microbiol. 78, 89–98. https://doi.org/10.1128/AEM.06017-11.

Kessler, R.C., Sampson, N.A., Berglund, P., Gruber, M.J., Al-Hamzawi, A., Andrade, L., Bunting, B., Demyttenaere, K., Florescu, S., de Girolamo, G., Gureje, O., He, Y., Hu, C., Huang, Y., Karam, E., Kovess-Masfety, V., Lee, S., Levinson, D., Medina Mora, M.E., Moskalewicz, J., Nakamura, Y., Navarro-Mateu, F., Browne, M.A.O., Piazza, M., Posada-Villa, J., Slade, T., ten Have, M., Torres, Y., Vilagut, G., Xavier, M., Zarkov, Z., Shahly, V., Wilcox, M.A., 2015. Anxious and non-anxious major depressive disorder in the World Health Organization World mental Health surveys. Epidemiol. Psychiatr. Sci. 24, 210–226. https://doi.org/10.1017/S2045796015000189.

Kunjapur, A.M., Hyun, J.C., Prather, K.L.J., 2016. Deregulation of S-adenosylmethionine biosynthesis and regeneration improves methylation in the *E. coli de novo* vanillin biosynthesis pathway. Microb. Cell Factories 15, 61. https://doi.org/10.1186/s12934-016-0459-x.

Leung, A.Y., Paul, A.G., 1968. Baeocystin and norbaeocystin: new analogs of psilocybin from Psilocybe baeocystis. J. Pharm. Sci. 57, 1667–1671. https://doi.org/10.1002/JPS.2600571007.

Lin, Y., Sun, X., Yuan, Q., Yan, Y., 2014. Engineering Bacterial Phenylalanine 4-hydroxylase for Microbial Synthesis of Human Neurotransmitter Precursor 5-hydroxytryptophan, vol. 3. pp. 48. https://doi.org/10.1021/sb5002505.

Moisala, M.E., Rantamäki, T., Carthart-Harris, R., Nutt, D.J., 2017. Psilocybin and Depression (Psilo101). [WWW Document]. URL. https://clinicaltrials.gov/ct2/show/NCT03380442.

Passie, T., Seifert, J., Schneider, U., Emrich, H.M., 2002. The pharmacology of psilocybin. Addict. Biol. 7, 357–364. https://doi.org/10.1080/1355621021000005937.

Raison, C., 2019. A study of psilocybin for major depressive disorder (MDD). [WWW Document]. URL. https://clinicaltrials.gov/ct2/show/NCT03866174.

Romney, D.K., Murciano-Calles, J., Wehrmüller, J.E., Arnold, F.H., 2017. Unlocking reactivity of TrpB: a general biocatalytic platform for synthesis of tryptophan analogues. J. Am. Chem. Soc. 139, 10769–10776. https://doi.org/10.1021/jacs.7b05007.

Ross, S., Bossis, A., Guss, J., Agin-Liebes, G., Malone, T., Cohen, B., Mennenga, S.E., Belser, A., Kalliontzi, K., Babb, J., Su, Z., Corby, P., Schmidt, B.L., 2016. Rapid and sustained symptom reduction following psilocybin treatment for anxiety and depression in patients with life-threatening cancer: a randomized controlled trial. J. Psychopharmacol. 30, 1165–1180. https://doi.org/10.1177/0269881116675512.

Shirota, O., Hakamata, W., Goda, Y., 2003. Concise large-scale synthesis of psilocin and psilocybin, principal hallucinogenic constituents of "Magic Mushroom". J. Nat. Prod. 66, 885–887. https://doi.org/10.1021/np030059u.

Studier, F.W., 2005. Protein production by auto-induction in high-density shaking cultures. Protein Expr. Purif. 41, 207–234. https://doi.org/10.1016/j.pep.2005.01.016.

Sun, X., Lin, Y., Yuan, Q., Yan, Y., 2015. Precursor-directed biosynthesis of 5-hydroxytryptophan using metabolically engineered *E. coli*. ACS Synth. Biol. 4, 554–558. https://doi.org/10.1021/sb500303q.

Tylš, F., Páleníček, T., Horáček, J., 2014. Psilocybin – summary of knowledge and new perspectives. Eur. Neuropsychopharmacol. 24, 342–356. https://doi.org/10.1016/j.euroneuro.2013.12.006.

van den Berg, E.M.M., Jansen, F.J.H.M., de Goede, A.T.J.W., Baldew, A.U., Lugtenburg, J., 2010. Chemo-enzymatic synthesis and characterization of L-tryptophans selectively 13C-enriched or hydroxylated in the six-membered ring using transformed *Escherichia coli* cells. Recl. des Trav. Chim. des Pays-Bas. 109, 287–297. https://doi.org/10.1002/recl.19901090405.

Wilcox, M., 1974. The enzymatic synthesis of l-tryptophan analogues. Anal. Biochem. 59, 436–440. https://doi.org/10.1016/0003-2697(74)90296-6.

Wu, G., Yan, Q., Jones, J.A., Tang, Y.J., Fong, S.S., Koffas, M.A.G., 2016. Metabolic burden: cornerstones in synthetic biology and metabolic engineering applications. Trends Biotechnol. 34, 652–664. https://doi.org/10.1016/j.tibtech.2016.02.010.

Wu, J., Du, G., Zhou, J., Chen, J., 2013a. Metabolic engineering of *Escherichia coli* for (2S)-pinocembrin production from glucose by a modular metabolic strategy. Metab. Eng. 16, 48–55. https://doi.org/10.1016/j.ymben.2012.11.009.

Wu, J., Liu, P., Fan, Y., Bao, H., Du, G., Zhou, J., Chen, J., 2013b. Multivariate modular metabolic engineering of *Escherichia coli* to produce resveratrol from l-tyrosine. J. Biotechnol. 167, 404–411. https://doi.org/10.1016/j.jbiotec.2013.07.030.

Xu, P., Gu, Q., Wang, W., Wong, L., Bower, A.G.W., Collins, C.H., Koffas, M.A.G., 2013a. Modular optimization of multi-gene pathways for fatty acids production in *E. coli*. Nat. Commun. 4. https://doi.org/10.1038/ncomms2425.

Xu, P., Gu, Q., Wang, W., Wong, L., Bower, A.G.W., Collins, C.H., Koffas, M.A.G., 2013b. Modular optimization of multi-gene pathways for fatty acids production in *E. coli*. Nat. Commun. 4, 1409. https://doi.org/10.1038/ncomms2425.

Xu, P., Vansiri, A., Bhan, N., Koffas, M.A.G., 2012. ePathBrick: a synthetic biology platform for engineering metabolic pathways in *E. coli*. Biol. 1, 256–266. https://doi.org/10.1021/sb300016b.